A flux form, semi - Lagrangian method for the scalar advection equation using Discontinuous Galerkin reconstruction

Marco Restelli [a], *Luca Bonaventura* [a], *Riccardo Sacco* [b]

[a]MOX– Modellistica e Calcolo Scientifico,
Dipartimento di Matematica "F. Brioschi",
Politecnico di Milano, via Bonardi 9, 20133 Milano, Italy

[b]Dipartimento di Matematica "F. Brioschi",
Politecnico di Milano, via Bonardi 9, 20133 Milano, Italy

Keywords: Advection equation, tracer transport, semi–Lagrangian techniques, Discontinuous Galerkin finite element method.

AMS Subject Classification: 65M25, 65M60, 68W10, 86A10

Abstract

A new semi-Lagrangian formulation is proposed for the discretization of the scalar advection equation in flux form. The approach combines the accuracy and flexibility of the Discontinuous Galerkin method with the computational efficiency and robustness of Semi-Lagrangian techniques. Unconditional stability of the proposed discretization is proven in the von Neumann sense for the one dimensional case. A monotonization technique is then introduced, based on the Flux Corrected Transport approach. This yields a multidimensional monotonic scheme for the piecewise constant component of the computed solution, while reducing the numerical diffusion of monotonization approaches more common in the Discontinuous Galerkin framework. The accuracy and stability of the method are further demonstrated by two dimensional tracer advection tests. The comparison with results obtained by standard semi - Lagrangian and Discontinuous Galerkin methods highlights several computational advantages of the new technique.

1 Introduction

The development of accurate and conservative numerical methods to solve efficiently the linear advection equation

$$\frac{\partial c}{\partial t} + \nabla \cdot (\mathbf{u}c) = 0 \tag{1}$$

has always been a main goal of the research on advection dominated flows. In many important applications, especially in environmental modelling, the solution of large system of advection - diffusion - reaction equations requires an increasingly large share of the available computational time. For example, atmospheric chemistry, air quality, water quality or ocean biogeochemistry models require the solution of one advection - diffusion - reaction equation for each chemical or biological species involved, whose number can be quite high (see e.g. the atmospheric chemistry and aerosol models described in [23], [44]), if a detailed description of the processes of interest has to be achieved. Thus, very efficient numerical methods are crucial to perform long range simulations effectively. Furthermore, good scalability and parallel efficiency are also essential requirements for these computationally intensive applications. These equations are usually coupled only by the reaction terms, while their advection and diffusion components are essentially decoupled.

In the context of these low Mach number, advection dominated flows, the semi - Lagrangian method (also known as modified method of characteristics, Eulerian - Lagrangian method or the characteristic Galerkin method in different modelling communities, see, e.g., the reviews in [13], [33], [42]) is widely acknowledged as an accurate and efficient option. The original formulation of semi - Lagrangian methods, however, is inherently non conservative. The advection equation (1) is reformulated in Lagrangian form

$$\frac{dc}{dt} = \frac{\partial c}{\partial t} + \mathbf{u} \cdot \nabla c = 0 \tag{2}$$

and time discretization exploits the fact that the solution values are constant along the characteristic lines, which are approximated numerically (see e.g. [41] for a discussion of the issues related to this approximation). For simplicity of the presentation, we assume in the following to deal with incompressible flows only, but most of the ideas that we will discuss generalize naturally to the compressible case.

A number of approaches have been proposed to overcome the lack of mass conservation of semi - Lagrangian methods. In many practical applications, *a posteriori* mass restoration is performed to keep the mass of the atmosphere constant. The methods proposed in [20], [36] enforce mass conservation as a global constraint, which is however still achieved via redistribution of the mass gains or losses among all mesh points. Neither of these simpler approaches guarantees local mass conservation, i.e., changes in the solution at a given mesh point do not necessarily depend only on the values at the neighbouring mesh points.

In order to achieve also local mass conservation, two main strategies have been pursued. In the first strategy, the advection equation (2) is

integrated over a volume $\Omega(t)$ that is moving with the flow, in order to obtain

$$\frac{d}{dt}\int_{\Omega(t)} c(x,t)\ dx = 0. \tag{3}$$

Taking $\Omega(t+\Delta t)$ to coincide with a mesh control volume, as in the non conservative semi - Lagrangian approach, time integration of (3) yields

$$\int_{\Omega(t+\Delta t)} c(x,t)\ dx = \int_{\Omega(t)} c(x,t)\ dx, \tag{4}$$

where $\Omega(t)$ is now the upstream control volume which evolves into $\Omega(t+\Delta t)$ within the timestep Δt (see Fig. 1). Equation (4) is then discretized by approximate reconstruction of the upstream control volume and approximate computation of the integral on the right hand side. This approach has been sometimes called conservative remapping, or cell integrated semi - Lagrangian method. The idea of remapping dates back at least to [22]. Mass conserving variants of the semi - Lagrangian method based on this concept of remapping were introduced for example in [25], [30], [31], [35].

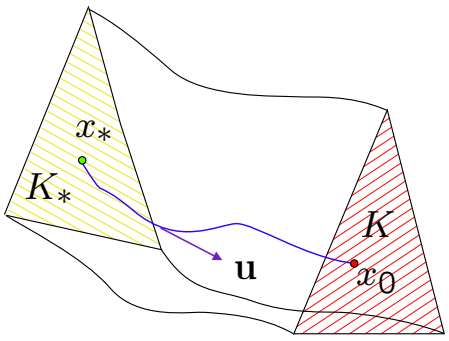

Figure 1: The upstream control volume used in advective form conservative extensions of semi-Lagrangian schemes.

In the second strategy, that is more similar in spirit to Eulerian finite volume methods, equation (1) is integrated in space over a fixed mesh control volume Ω and the divergence theorem is applied as usual. The resulting equation is then integrated in time over a generic time step Δt, in order to obtain

$$\begin{aligned}\int_{\Omega} c(x,t+\Delta t)\ dx \quad &= \int_{\Omega} c(x,t)\ dx \\ &- \int_t^{t+\Delta t} ds \int_{\partial\Omega} c(\xi,s)\mathbf{u}(\xi,s)\cdot\mathbf{n}\ d\xi.\end{aligned} \tag{5}$$

Equation (5) is then discretized by approximate reconstruction of the flux through the domain boundary $\partial\Omega$ over the time step Δt, see Fig. 2, where Ω is assumed to coincide with a mesh element K and the *flux tube* based

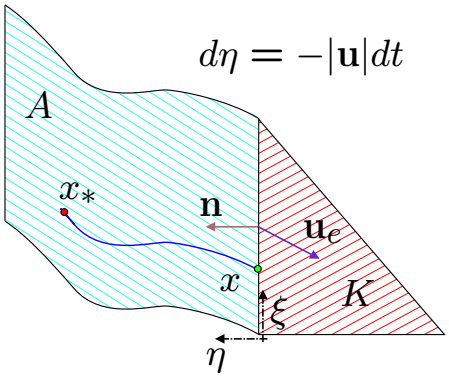

Figure 2: The *flux tube* used in flux form conservative extensions of semi-Lagrangian schemes.

on a portion of ∂K is represented. Semi-Lagrangian backward trajectories that reach a number of points along ∂K at time $t + \Delta t$ are computed and used for the approximation of the fluid portion that is advected through the boundary. Some form of polynomial reconstruction is then used at these points to discretize the space time integral on the right–hand side. We will refer loosely to methods which can be described in this way as flux form semi - Lagrangian methods. Examples of these techniques have been introduced for example in [12], [15], [16], [17], [18], [19], [26], [28], [29]. In [33], these approaches were described in a wider context as generalized Godunov methods and a stability analysis was outlined. It should be remarked that generalized Godunov methods can also be interpreted as a natural generalization of the so called wave propagation methods, see e.g. [27].

The purpose of the present work is to introduce a flux form semi - Lagrangian discretization for the scalar advection equation that employs a Discontinuous Galerkin (DG) formulation (see e.g. [10]) to reconstruct the numerical solution within each control volume. We will refer shortly to this technique as semi - Lagrangian Discontinuous Galerkin (SLDG) approach. More specifically, discontinuous elements are used to reconstruct the numerical solution at the points needed for the computation of the space time integral in (5). In doing so, the proposed method aims at combining the accuracy and locality of the DG method with the computational efficiency and robustness of semi - Lagrangian techniques. The use of semi - Lagrangian backward trajectories allows to achieve unconditional stability, irrespective of the value of the Courant number. This overcomes the rather stringent stability restricitions required by the DG scheme. In the case of large systems of advection - diffusion - reaction equations, the extra computational effort needed to compute the trajectories is required only once for the whole system, thus reducing the potential overhead associated with this procedure. The proposed method also appears to exhibit several advantages in a massively parallel computing framework. Firstly, the

type and amount of information that different processors need to exchange within one time step can be estimated only once for the whole system. This feature is also shared by the approaches presented in [25], [30], [31], [35]. The present approach, however, would have peculiar features similar to those of the Eulerian DG formulation, since higher order reconstructions could be achieved without using large stencils, thus making domain decomposition parallelization approaches more straightforward. Furthermore, the potential loss of accuracy of standard semi-Lagrangian methods at low Courant numbers that was highlighted in [14] does not affect the method we propose.

A brief outline of the article is as follows. The SLDG method is described in greater detail in Sect. 2. A von Neumann stability analysis for the constant coefficient, one dimensional case is then carried out in Sect. 3, showing that the method is stable for arbitrary Courant number. Since the SLDG is not inherently monotonic in its higher order version, a monotonization approach based on the Flux Corrected Transport (FCT) technique is introduced and discussed in Sect. 4, while in Sect. 5 the interesting properties of the new method are demonstrated by a number of numerical tests relevant in advection dominated flows. The issue of coupling with discrete models of divergent or variable density flow is discussed in section Sect. 6, while future developments and possible applications are discussed in Sect. 7.

2 The Semi-Lagrangian Discontinuous Galerkin method

In this section we describe in greater detail the Semi-Lagrangian Discontinuous Galerkin (SLDG) method. In doing this, we combine the unified framework for generalized Godunov methods proposed in [33] with the Discontinuous Galerkin finite element formulation introduced and analyzed in [8], [10] in the case of nonlinear hyperbolic problems.

2.1 Notation

Firstly, the basic notation used for the discretization of the linear advection problem (1) is introduced. For simplicity, we assume henceforth that Ω is an open bounded domain of $\mathbb{R}^2$, and let $\mathcal{T}_h$ denote a triangulation of Ω into N_{el} triangular elements K, although the method can be easily extended to deal with three-dimensional problems and to include quadrilateral elements as well. The area of an element is denoted by $|K|$, while its boundary and outward unit normal vector are ∂K and $\mathbf{n}_{\partial K}$, respectively. The set of all the edges of K is $\mathcal{E}_K$, while $\mathcal{E}_h$ is the set of the N_{edges} edges of the triangulation, with $|e|$ denoting the length of a generic edge $e \in \mathcal{E}_h$ and $\mathbf{n}_e$ being a normal unit vector arbitrarily associated with edge e. For each element and edge, an orientation $\sigma_{K,e} = \pm 1$ is also defined, so that $\sigma_{K,e}\mathbf{n}_e$ is the outer normal unit vector associated with edge e of element K. We will also denote by u_e the discrete value of the normal velocity component in the direction of $\mathbf{n}_e$, u_e being a constant quantity over each edge $e \in \mathcal{E}_h$.

Equation (1) will be solved on Ω with appropriate inflow boundary conditions and assuming that a smooth, incompressible velocity field is given. In order to make coupling to generic hydrodynamic models more straightforward, the velocity field is assumed to be known in discrete form only and to satisfy the discrete divergence free constraint exactly. More specifically, for each time interval $[t^n, t^{n+1}]$, with $\Delta t = t_{n+1} - t_n$, the components of the velocity field normal to the edges of $\mathcal{T}_h$ are assumed to be given at a single intermediate time level $t^{n+\frac{1}{2}}$. These components will be denoted by $u_e^{n+\frac{1}{2}}, e = 1, \ldots, N_{edges}$, although the time dependence will often be omitted for the sake of simplicity. The discrete divergence free constraint amounts to requiring the following equation to be satisfied for each element $K \in \mathcal{T}_h$

$$\sum_{e \in \mathcal{E}_K} \sigma_{K,e} u_e^{n+\frac{1}{2}} |e| = 0. \tag{6}$$

Although the above assumption on $u_e^{n+\frac{1}{2}}$ reduces *a priori* the formal time accuracy of the method to second order, it corresponds to what is actually computationally feasible when coupling tracer advection to most semi-Lagrangian models for fluid flow. This assumption also helps to ease the future coupling of the proposed method to mass conservative methods for environmental flows, such as those proposed in [4], [5], [6], [32]. As a matter of fact, these numerical methods use the discrete normal components u_e as prognostic variables and employ Raviart-Thomas finite elements (see e.g. [37]) to reconstruct the velocity field from these components. Furthermore, the present framework can be seen as an extension to triangular grids of the C-type staggering commonly used on Cartesian grids in many environmental models (see e.g. [1]). Thus, this choice should allow a natural application of the proposed SLDG method in a wide number of already available models. It is to be remarked that appropriate coupling of the mass continuity equation and flux form tracer equations is essential for accurate transport modelling. The issue of discrete *consistency with continuity* has been highlighted by many authors and the inaccuracies resulting from neglecting this issue have been analyzed in [21]. In the present, preliminary stage, the velocity field is assumed to be divergence free for simplicity of the presentation. However, the generalization to the divergent case is being investigated and the outline of a general proof of discrete consistency with continuity will be introduced in Sect. 6.

2.2 Spatial discretization

The spatial discretization of (1) is carried out initially along the usual lines of Discontinous Galerkin (DG) methods (see e.g. [8]). In this preliminary presentation, only piecewise linear elements will be considered for simplicity. It is to be remarked that, in principle, the order of the polynomials used could be different for each element $K \in \mathcal{T}_h$. As it will be clear from the description of the numerical method, this can be done maintaining the global and local mass conservation properties of the scheme. This more general case will not be considered here for the sake of simplicity, but it

will be exploited in a forthcoming implementation to reduce computational costs.

An approximation $c_h = c_h(x,t)$ to the solution $c(x,t)$ of (1) is sought, such that c_h is a linear polynomial over each element $K \in \mathcal{T}_h$ for each time t, not necessarily continuous across the edges of K. Multiplying equation (1) by a piecewise linear function v_h, integrating over $K \in \mathcal{T}_h$ and replacing the exact solution c by its approximation c_h, one obtains

$$\int_K \frac{\partial c_h}{\partial t}\, v_h(x)\, dx = -\int_K \mathrm{div}(\mathbf{u}\, c_h)\, v_h(x)\, dx \qquad \forall K \in \mathcal{T}_h.$$

Then, formally integrating by parts, we obtain

$$\int_K \frac{\partial c_h}{\partial t}\, v_h(x)\, dx = \int_K \mathbf{u}\cdot\nabla v_h(x)\, dx - \int_{\partial K} c_h \mathbf{u}\cdot\mathbf{n}_{\partial K}\, d\xi \qquad \forall K \in \mathcal{T}_h. \quad (7)$$

Notice that the advective boundary term $c_h(\xi,t)\mathbf{u}\cdot\mathbf{n}_{\partial K}$ in (7) does not yet have a precise meaning, because c_h is a discontinuous function across interelement boundaries. Equation (7) is the starting point for time discretization with Runge-Kutta schemes in standard DG formulations [8], [10]. In our approach, we depart from this latter procedure and follow the path of generalized Godunov methods as presented and analized in [33]. With this aim, we integrate (7) in time between t^n and t^{n+1}, to obtain the following weak form of the linear advection equation

$$\begin{aligned}
&\int_K c_h(x,t^{n+1})\, v_h(x)\; dx = \int_K c_h(x,t^n)\, v_h(x)\; dx \\
&+ \int_{t^n}^{t^{n+1}} ds \int_K c_h(x,s)\, \mathbf{u}\cdot\nabla v_h\, dx \qquad (8)\\
&- \int_{t^n}^{t^{n+1}} ds \int_{\partial K} c_h(\xi,s)\, \mathbf{u}\cdot\mathbf{n}_{\partial K}\, v_h(\xi)\, d\xi \qquad \forall K \in \mathcal{T}_h.
\end{aligned}$$

For simplicity, we will restrict ourselves to the case of piecewise linear polynomials, but the method can be easily extended to more general polynomial spaces. For each element K, the discrete degrees of freedom associated with a numerical solution at a given timestep t^n are denoted by $\mathbf{c}_K^n = \{c_{j,K}^n\}_{j=0}^2$, so that an approximate numerical solution can be reconstructed locally for all $K \in \mathcal{T}_h$ as

$$c_{h,K}(x,t^n) \equiv c_{h,K}^n(x) = c_{0,K}^n \phi_0(x) + c_{1,K}^n \phi_1(x) + c_{2,K}^n \phi_2(x), \qquad (9)$$

where $\phi_0(x), \phi_1(x), \phi_2(x)$ are taken to be an orthogonal basis for the linear polynomials over K such that $\int_K \phi_i(x)\phi_j(x)dx = |K|\delta_{ij}$ (and, in particular, $\int_K \phi_1(x)dx = \int_K \phi_2(x)dx = 0$ and $\phi_0(x) = \mathbb{1}_K(x)$, where $\mathbb{1}_K$ is the characteristic function associated with element K).

The approximate numerical solution for all $x \in \Omega$ at the time level t^n reads then

$$c_h(x,t^n) \equiv c_h^n(x) = \sum_{K\in\mathcal{T}_h} \sum_{j=0}^{2} c_{j,K}^n \phi_j(x).$$

2.3 Time discretization

The next step is to derive from (8) a full space-time discretization. In order to describe the time evolution of $c_h(x,t)$, we define, as in [33], the exact evolution operator

$$E(t^n,\Delta t) : c(x,t^n) \to [E(t^n,\Delta t)c(\cdot,t^n)](x) = c(x,t^n+\Delta t). \tag{10}$$

$E(t^n,\Delta t)$ can be interpreted as a representation of the solution of the linear advection equation *in non conservative* form (2). More precisely, under mild regularity assumptions on the velocity field (see e.g. the discussion in [37]), it can be proven that streamline or characteristic line functions exist, which are defined as the solutions of the ordinary differential equations

$$\frac{d}{d\tau}X(x,t;\tau) = \mathbf{u}(X(x,t;\tau),\tau) \tag{11}$$

with initial datum at time t given by $X(x,t;t) = x$. For smooth initial data, by the chain rule it is then possible to prove that for any t and τ the following relation holds

$$c(x,t) = [E(\tau,t-\tau)c(.,\tau)](x) = c(X(x,t;\tau),\tau). \tag{12}$$

A discrete approximation of this evolution operator representing the time evolution from t^n to $t^n+\Delta t$ will be denoted by $E^n_{\Delta t}$. This approximation is completely determined once a discrete approximation $\widehat{X}(x,t;\tau)$, with $\tau \in [t^n, t^n+\Delta t]$, is provided for the solution of (11). The latter can be interpreted as the numerical approximation of the streamlines usually performed in semi - Lagrangian methods. It can be assumed that all the basic semigroup properties of the continuous evolution operator, such as equation (12), still hold for its discrete approximation, so that, for example, we can write

$$[E^n_s c^n_h](x) = c^n_h(\widehat{X}(x,t^n+s;t^n)), \tag{13}$$

with $s \in [0,\Delta t]$. Following the ideas proposed e.g. in [26], [28], we can now resort to (12) and the operator $E^n_{\Delta t}$ to evaluate the right hand side of (8). More precisely, the SLDG method can be defined for each element $K \in \mathcal{T}_h$ by

$$\begin{aligned} |K|\, c^{n+1}_{i,K} \quad &= |K|\, c^n_{i,K} \\ &+ \int_0^{\Delta t} ds \int_K [E^n_s c^n_h](x)\, \mathbf{u}(x,t^n)\cdot\nabla\phi_i(x)\, dx \\ &- \int_0^{\Delta t} ds \sum_{e\in\mathcal{E}_K} \int_e [E^n_s c^n_h](\xi)\, u_e\, \phi_i(\xi)\, d\xi, \\ &i = 0,\ldots,2. \end{aligned} \tag{14}$$

2.4 The fully discrete SLDG approximation

In order to obtain a fully discrete method, the integrals in space and time in (14) must be replaced by appropriate quadrature rules. In the present implementation of the proposed method, Gaussian quadrature rules have been used for the integration in space. Normalized Gaussian points $\{x_v\}_{v=1}^{L_e}$, $\{y_v\}_{v=1}^{L_f}$, are introduced according to some parametric representation of the edges and the elements, respectively. The corresponding Gaussian weights are denoted by $\{\tilde{\omega}_v\}_{v=1}^{L_e}$, $\{\tilde{\tilde{\omega}}_v\}_{v=1}^{L_f}$. For the integration in time, a simple composite rule is applied in the present implementation. For each element K and for each edge e, we define intermediate time levels $\{s_m^K\}_{m=0}^{M(K)}$, $\{s_m^e\}_{m=0}^{M(e)}$. For convenience, the dependency on the edge and element will often be dropped and should be recovered from the context. The intermediate time steps are such that $s_0 = 0$, $s_M = \Delta t$ and $\Delta\tau_m = s_m - s_{m-1}$. Formally, we will make the approximation

$$\int_0^{\Delta t} E_s^n \, ds \approx \sum_{m=0}^{M-1} E^n_{s_{m+\frac{1}{2}}} \Delta\tau_m, \tag{15}$$

where now $s_{m+\frac{1}{2}} = s_m + \frac{\tau_m}{2}$. More accurate composite integration rules can of course be used along the same lines. The numerical trajectories $\widehat{X}(x, t^n + s; t^n)$ necessary for the complete definition of E_s^n are computed by a simple backward Euler method with time substeps given by the τ_m. Given these definitions, the fully discrete SLDG approximation of equation (1) can then be defined for each $K \in \mathcal{T}_h$ as

$$\begin{aligned} |K| c_{i,K}^{n+1} \quad &= |K| c_{i,K}^n \\ &+ \sum_{m=0}^{M-1} \sum_{v=1}^{L_f} [E^n_{s_{m+\frac{1}{2}}} c_h^n](y_v) \mathbf{u}(y_v, t^n) \cdot \nabla\phi_i(y_v) \, \Delta\tau_m \, \tilde{\tilde{\omega}}_v \\ &- \sum_{e \in \mathcal{E}_K} \sigma_{K,e} u_e \, |e| \sum_{m=0}^{M-1} \sum_{v=1}^{L_e} [E^n_{s_{m+\frac{1}{2}}} c_h^n](x_v) \, \phi_i(x_v) \, \Delta\tau_m \, \tilde{\omega}_v, \\ &i = 0, \ldots, 2. \end{aligned} \tag{16}$$

It is to be remarked that the approximation (15) of the evolution operator eliminates the ambiguity in the definition of the numerical fluxes along interelement boundaries, since in all cases with non zero advecting velocity the quantity $[E^n_{s_{m+\frac{1}{2}}} c_h^n](x_v)$ is univocally defined for $m = 0, \cdots, M-1$. In the special case where piecewise constant finite elements are considered, the following finite volume method is recovered

$$\begin{aligned} |K| \, c_{0,K}^{n+1} \quad &= |K| \, c_{0,K}^n \\ &- \sum_{e \in \mathcal{E}_K} \sigma_{K,e} u_e \, |e| \sum_{m=0}^{M-1} \sum_{v=1}^{L_e} [E^n_{s_{m+\frac{1}{2}}} c_h^n](x_v) \, \Delta\tau_m \, \tilde{\omega}_v, \end{aligned} \tag{17}$$

where the quantity $c_{0,K}^n$ is the discrete degree of freedom representing the average of the concentration over element $K \in \mathcal{T}_h$ and c_h^n is a piecewise constant function over $\mathcal{T}_h$.

3 Linear stability analysis in the one-dimensional case

The von Neumann stability analysis of the SLDG scheme will now be carried out along the lines of [7]. With this aim, let us consider equation (1) in the one dimensional case with constant advection velocity

$$\begin{cases} c_t + uc_x = 0 & \text{in} \quad [0\,,\,L] \times [0\,,\,T] \\ c(x,0) = c_0(x) & x \in [0\,,\,L], \end{cases} \tag{18}$$

and supplied with periodic initial and boundary conditions. Let $\mathcal{T}_h$ be a uniform triangulation of $[0\,,\,L]$, with h denoting the (uniform) amplitude of each element $K \in \mathcal{T}_h$ and Δt denoting the time step. Finally, for each $K_i \in \mathcal{T}_h$, let x_i, $x_{i+\frac{1}{2}}$ and $x_{i-\frac{1}{2}}$ be the midpoint and the points on the boundary of K_i, respectively. The key stability parameter is the Courant number $C = \frac{u\Delta t}{h}$, which can be split in its integer and fractional part

$$C = m + \gamma, \qquad m \in \mathbb{N}, \quad \gamma \in [0\,,\,1),$$

as customary in the analysis of semi-Lagrangian schemes (see e.g. [2]). Introducing the cell characteristic time $\tau = \frac{h}{u}$ we have also

$$\Delta t = (m+\gamma)\tau.$$

Denoting now by a_i and b_i the degrees of freedom with respect to the $\mathbb{P}_1$ hierarchical basis, the approximate concentration c_h is given at any time level t^n by

$$c_h^n(x)|_{K_i} = a_i^n + b_i^n(x - x_i) \qquad \forall K_i \in \mathcal{T}_h.$$

Then, the SLDG formulation for the evolution from time level t^n to t^{n+1} reads

$$\begin{aligned} a_i^{n+1} &= a_{i-m}^n - \gamma\left[a_{i-m}^n - a_{i-m-1}^n + \frac{1}{2}h(1-\gamma)(b_{i-m}^n - b_{i-m-1}^n)\right] \qquad (19) \\ b_i^{n+1} &= b_{i-m}^n + 6\gamma(1-\gamma)\frac{a_{i-m}^n - a_{i-m-1}^n}{h} - \gamma\Big[3(1-\gamma)(b_{i-m}^n + b_{i-m-1}^n) \\ &\quad +2\gamma\left(\frac{3}{2} - \gamma\right)(b_{i-m}^n - b_{i-m-1}^n)\Big] \end{aligned}$$

or, equivalently

$$\begin{aligned} a_i^{n+1} &= a_{i-m}^n - \gamma(a_{i-m}^n - a_{i-m-1}^n) \qquad (20) \\ &\quad -\sqrt{3}\gamma(1-\gamma)(s_{i-m}^n - s_{i-m-1}^n) \\ s_i^{n+1} &= s_{i-m}^n + \sqrt{3}\gamma(1-\gamma)(a_{i-m}^n - a_{i-m-1}^n) \\ &\quad -3\gamma(1-\gamma)(s_{i-m}^n + s_{i-m-1}^n) - 2\gamma^2\left(\frac{3}{2} - \gamma\right)(s_{i-m}^n - s_{i-m-1}^n) \end{aligned}$$

where the new degrees of freedom

$$s_i^n = \frac{\sqrt{3}h}{6}b_i^n$$

have been introduced for the purpose of simplifying the stability analysis. Equations (19)-(20) can be obtained as follows. Taking in (8) $v_h = \phi_0(x) = \mathbb{1}_{K_i}$ yields

$$h(a_i^{n+1} - a_i^n) = \int_{t^n}^{t^{n+1}} \mathrm{d}t\, u(-\xi_{i+\frac{1}{2}} + \xi_{i-\frac{1}{2}})$$

where $\xi_{i+\frac{1}{2}}$ represents the value of $E_{\Delta t}^n c_h$ in $x_{i+\frac{1}{2}}$ (see Fig. 3). For this analysis, we will assume that $E_{\Delta t}^n c_h$ coincides with the exact evolution operator, so that

$$\xi_{i+\frac{1}{2}} = c_h^n(x_{i+\frac{1}{2}} - u\Delta t) \tag{21}$$

Then, evaluating the integral

$$\begin{aligned} ha_i^{n+1} - ha_i^n \quad &= u\left\{\sum_{k=1}^{m}\int_{t^n+(k-1)\tau}^{t^n+k\tau} -\xi_{i+\frac{1}{2}}\mathrm{d}t + \int_{t^n+m\tau}^{t^n+\Delta t} -\xi_{i+\frac{1}{2}}\mathrm{d}t\right. \\ &\left. + \sum_{k=1}^{m}\int_{t^n+(k-1)\tau}^{t^n+k\tau} \xi_{i-\frac{1}{2}}\mathrm{d}t + \int_{t^n+m\tau}^{t^n+\Delta t} \xi_{i-\frac{1}{2}}\mathrm{d}t\right\} \\ &= u\tau\left\{-\sum_{k=1}^{m} a_{i-k+1}^n - \gamma\left[a_{i-m}^n + \frac{h}{2}(1-\gamma)b_{i-m}^n\right] + \sum_{k=1}^{m} a_{i-k}^n\right. \\ &\left. +\gamma\left[a_{i-m-1}^n + \frac{h}{2}(1-\gamma)b_{i-m-1}^n\right]\right\} \\ &= u\tau\left\{a_{i-m}^n - a_i^n - \gamma\left[a_{i-m}^n - a_{i-m-1}^n + \frac{h}{2}(1-\gamma)(b_{i-m}^n - b_{i-m-1}^n)\right]\right\} \end{aligned} \tag{22}$$

gives the first equation in (19) after further algebraic manipulation.

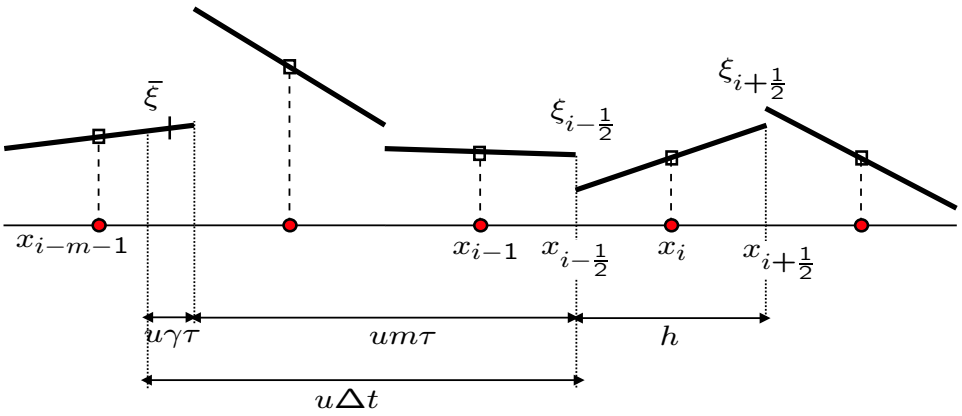

Figure 3: Piecewise linear solution of the advection equation in the one dimensional case with constant coefficients.

Taking now in (8) $v_h = \phi_1(x) = (x - x_i)\mathbb{1}_{K_i}$ we obtain

$$\frac{h^3}{12}(b_i^{n+1} - b_i^n) = \int_{t^n}^{t^{n+1}} \mathrm{d}t\, u\left[-\xi_{i+\frac{1}{2}}\frac{h}{2} + \xi_{i-\frac{1}{2}}\left(-\frac{h}{2}\right) + \int_{K_i} E_\Delta c_h^n\,\mathrm{d}x\right],$$

which yields, after decomposing the time integrals

$$\begin{aligned}\frac{h^3}{12}b_i^{n+1}-\frac{h^3}{12}b_i^n \quad &= u\left\{-\frac{h}{2}\left[\sum_{k=1}^{m}\int_{t^n+(k-1)\tau}^{t^n+k\tau}\xi_{i+\frac{1}{2}}\mathrm{d}t\right.\right. \\ &+\left.\int_{t^n+m\tau}^{t^n+\Delta t}\xi_{i+\frac{1}{2}}\mathrm{d}t+\sum_{k=1}^{m}\int_{t^n+(k-1)\tau}^{t^n+k\tau}\xi_{i-\frac{1}{2}}\mathrm{d}t+\int_{t^n+m\tau}^{t^n+\Delta t}\xi_{i-\frac{1}{2}}\mathrm{d}t\right] \\ &+\left.\sum_{k=1}^{m}\int_{t^n+(k-1)\tau}^{t^n+k\tau}\mathrm{d}t\int_{K_i}E_\Delta c_h^n\,\mathrm{d}x+\int_{t^n+m\tau}^{t^n+\Delta t}\mathrm{d}t\int_{K_i}E_\Delta c_h^n\,\mathrm{d}x\right\}.\end{aligned} \tag{23}$$

Substituting now (21) in (23) we obtain

$$\begin{aligned}\frac{h^3}{12}b_i^{n+1}-\frac{h^3}{12}b_i^n \quad &= u\left\{-\frac{1}{2}h\tau\sum_{k=1}^{m}\left(a_{i-k+1}^n+a_{i-k}^n\right)\right. \\ &-\frac{1}{2}h\tau\gamma\left(a_{i-m}^n+a_{i-m-1}^n+\frac{h}{2}(1-\gamma)(b_{i-m}^n+b_{i-m-1}^n)\right) \\ &+\frac{1}{2}h\tau\sum_{k=1}^{m}\left(a_{i-k}^n+a_{i-k+1}^n\right)+\frac{1}{12}h^2\tau\sum_{k=1}^{m}\left(b_{i-k}^n-b_{i-k+1}^n\right) \\ &+\frac{1}{2}h\tau\gamma^2a_{i-m-1}^n+h\tau\gamma\left(1-\frac{1}{2}\gamma\right)a_{i-m}^n \\ &+\left.\frac{1}{2}h^2\tau\gamma^2\left(\frac{1}{2}-\frac{1}{3}\gamma\right)(b_{i-m-1}^n-b_{i-m}^n)\right\}\end{aligned} \tag{24}$$

which, after some further algebraic manipulation, gives the second equation in (19).

At each time level, the approximate (periodic) solution c_h^n is represented via the degrees of freedom a_i, s_i. Because of the definition of s_i we obtain

$$||c_h^n||_{L^2(0,L)}^2=h\sum_i\{(a_i^n)^2+(s_i^n)^2\}. \tag{25}$$

We can associate with each c_n^h the piecewise constant vector function $[a_h^n(x)\ s_h^n(x)]^T$ defined as

$$a_h^n(x)=\sum_i a_i^n\mathbb{1}_{K_i}(x),\qquad s_h^n(x)=\sum_i s_i^n\mathbb{1}_{K_i}(x)$$

and rewrite (25) as

$$||c_h^n||_{L^2(0,L)}^2=||a_h^n||_{L^2(0,L)}^2+||s_h^n||_{L^2(0,L)}^2. \tag{26}$$

We now consider the Fourier series associated with a_h^n and s_h^n:

$$a_h^n(x)=\sum_{k\in\mathbb{Z}}A_k^ne^{I\frac{2k\pi}{L}x},\qquad s_h^n(x)=\sum_{k\in\mathbb{Z}}S_k^ne^{I\frac{2k\pi}{L}x}\quad,$$

where $I=\sqrt{-1}$. Due to the Bessel-Parseval equality, we have

$$||a_h^n||_{L^2(0,L)}^2=L\sum_{k\in\mathbb{Z}}|A_k^n|^2,\qquad ||s_h^n||_{L^2(0,L)}^2=L\sum_{k\in\mathbb{Z}}|S_k^n|^2,$$

so that relation (26) implies

$$||c_h^n||^2_{L^2(0,L)} = L\sum_{k\in\mathbb{Z}}(|A_k^n|^2 + |S_k^n|^2). \tag{27}$$

The SLDG method allows to express the coefficient A_k^{n+1}, S_k^{n+1} as linear combinations of A_k^n, S_k^n as follows

$$\begin{bmatrix} A_k^{n+1} \\ S_k^{n+1} \end{bmatrix} = e^{-I\theta m}\mathbf{G}(\theta,\gamma)\begin{bmatrix} A_k^n \\ S_k^n \end{bmatrix} \tag{28}$$

where $\theta = \frac{2k\pi h}{L}$ and we have introduced the amplification matrix

$$\mathbf{G} = \begin{bmatrix} 1-\gamma(1-e^{-I\theta}) & -\sqrt{3}\gamma(1-\gamma)(1-e^{-I\theta}) \\ \sqrt{3}\gamma(1-\gamma)(1-e^{-I\theta}) & 1-3\gamma(1-\gamma)(1+e^{-I\theta})-\gamma^2(3-2\gamma)(1-e^{-I\theta}) \end{bmatrix}.$$

Let $\lambda_{1,2}$ denote the eigenvalues of $\mathbf{G}$, with $|\lambda_2| \le |\lambda_1|$. It can be checked that $\lambda_1 \neq \lambda_2 \quad \forall\theta \in [-\pi\,,\,\pi]$. Furthermore, for $\theta \to 0$ we have

$$|\lambda_1| = 1 - \frac{1}{72}\gamma(1-\gamma)(1-\gamma+\gamma^2)\theta^4 + \mathcal{O}(\theta^6)$$

and for arbitrary $\theta \in [-\pi\,,\,\pi]$ we have that $|\lambda_1|$ is always smaller than one for $|\gamma| \le 1$, as can be seen from the plots of λ_1, λ_2 in Fig. 3. This proves the unconditional stability of the SLDG method in the von Neumann sense.

This result is analogous to what is usually obtained for standard semi-Lagrangian methods (see e.g. [2], [14]), while it contrasts with the stability analysis carried out in [9], which yields the stability constraint $\gamma < \frac{1}{3}$ for the one dimensional case with linear basis functions.

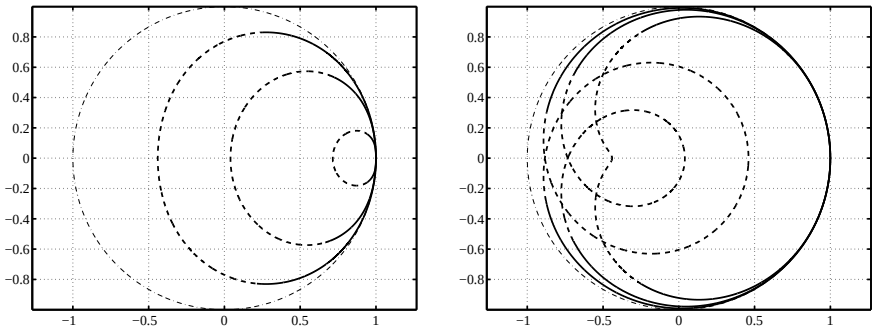

Figure 4: Representation of λ_1 (solid line) and λ_2 (dashed line) for $\gamma = 0.05,\ 0.2,\ 0.4$ (left) and $\gamma = 0.6,\ 0.8,\ 0.9$ (right). Dash–dot line: unit circle.

4 Monotonicity

In the context of DG methods for scalar conservation laws (see e.g. [8], [10]) a maximum principle is established by showing that the degrees of

freedom representing the average of the solution over each element K (i.e., in our case, the values $c_{0,K}^{n+1}$) are bounded by the maximum and minimum of $c_{0,K'}^{n}$, for every element $K' \in \mathcal{T}_h$ belonging to a neighbourhood of K. The proof of the above result is similar to the monotonicity proof for a finite volume scheme. In [10], the maximum principle for the DG method was proven by limiting the slopes of the numerical solution, represented by the degrees of freedom $c_{j,K}^{n}$, with $j = 1, 2$, in (9). In the present approach, instead, we enforce monotonicity by a suitable correction of the edge fluxes. We first introduce the functions

$$c_{h,j}^{n}(x) = \sum_{K \in \mathcal{T}_h} c_{j,K}^{n} \phi_{j,K}(x), \quad j = 0, 1, 2.$$

The contribution to the flux through edge e associated with the $j-$th degree of freedom can then be written as

$$F_e^j = u_e \, |e| \sum_{m=0}^{M-1} \sum_{v=1}^{L_e} [E^n_{s_{m+\frac{1}{2}}} c_{h,j}^{n}](x_v) \; \Delta\tau_m \, \tilde{\omega}_v, \quad j = 0, 1, 2.$$

This allows to reformulate the update for the mean (17) in the following equivalent form

$$\begin{aligned} c_{0,K}^{n+1} \quad &= c_{0,K}^{n} \\ &- \sum_{e \in \mathcal{E}_K} \frac{\sigma_{K,e} u_e \, |e|}{|K|} \sum_{m=0}^{M-1} \sum_{v=1}^{L_e} [E^n_{s_{m+\frac{1}{2}}} c_h^n](x_v) \; \Delta\tau_m \, \tilde{\omega}_v \\ &= - \sum_{e \in \mathcal{E}_K} \frac{\sigma_{K,e}}{|K|} F_e^0 - \sum_{j=1}^{2} \sum_{e \in \mathcal{E}_K} \frac{\sigma_{K,e}}{|K|} F_e^j. \end{aligned} \tag{29}$$

The monotonicity proof will then consist of two steps. First, it will be shown that the low order flux F_e^0 yields a monotonic method, given by

$$c_{0,K}^{n+1} = c_{0,K}^{n} - \sum_{e \in \mathcal{E}_K} \frac{\sigma_{K,e}}{|K|} F_e^0. \tag{30}$$

In the second step, a monotonic higher order method will be derived through the use of the well known Flux Corrected Transport (FCT) technique, (see e.g. [45]). In this approach, appropriate limiting coefficients $C_e \in [0, 1]$ are introduced for the antidiffusive fluxes F_e^1, F_e^2, so as to obtain the monotonized higher order scheme

$$c_{0,K}^{n+1} = c_{0,K}^{n} - \sum_{e \in \mathcal{E}_K} \frac{\sigma_{K,e}}{|K|} F_e^0 - \sum_{e \in \mathcal{E}_K} \frac{\sigma_{K,e}}{|K|} C_e \left[\sum_{j=1}^{2} F_e^j \right], \tag{31}$$

The derivation of the coefficients C_e is done exactly along the same lines as in the Cartesian grid case considered by [45], so the details of the computation of C_e will not be reported here.

We will now proceed to a reformulation of the low order flux F_e^0, in order to prove monotonicity of the low order method. More precisely, we

redefine F_e^0 as

$$F_e^0 = \int_0^{\Delta t} ds \int_e [E_s^n c_{h,0}^n](\xi)\ d\xi = \int_e d\xi \int_0^{\Delta t} [E_s^n c_{h,0}^n](\xi) ds. \qquad (32)$$

where we assume that, thanks to the piecewise constant structure of $c_{h,0}^n$, exact evaluation of the integrals is possible. Due to (13), one has

$$[E_s^n c_{h,0}^n](\xi) = c_{h,0}^n(\widehat{X}(\xi, t^n + s; t^n)),$$

from which

$$\int_0^{\Delta t} [E_s^n c_{h,0}^n](\xi)\ ds = \int_0^{\Delta t} c_{h,0}^n(\widehat{X}(\xi, t^n + s; t^n))\ ds.$$

It is to be remarked that, since the time dependency of the velocity field is assumed to be frozen during each time step, the set of points $\widehat{X}(\xi, t^n + s; t^n)$, $s \in [0\ ,\ \Delta t]$, coincides with those spanned by the backward trajectory $\widehat{X}(\xi, t^{n+1}; t^{n+1} - s)$, $s \in [0\ ,\ \Delta t]$.

Exploiting the fact that $c_{h,0}^n$ is piecewise constant over $\mathcal{T}_h$, the previous relation can be written as

$$\int_0^{\Delta t} c_{h,0}^n(\widehat{X}(\xi, t^n + s; t^n))\ ds = \sum_{K'} c_{0,K'}^n \Delta s_{K'}^{\xi},$$

where $\Delta s_{K'}^{\xi}$ denotes the amount of time during which $\widehat{X}(\xi, t^{n+1}; t^{n+1} - s) \in K'$ and the sum is extended over all elements crossed by $\widehat{X}(\xi, t^{n+1}; t^{n+1} - s)$. As a result, $\sum_{K'} \Delta s_{K'}^{\xi} = \Delta t$ independently of ξ and

$$F_e^0 = u_e |e| \Delta t \sum_{K' \in \mathcal{T}_e} \alpha_{K',e} c_{0,K'}^n, \qquad (33)$$

where we set

$$\alpha_{K',e} = \frac{1}{|e|\Delta t} \int_e \Delta s_{K'}^{\xi}\ d\xi \qquad (34)$$

and where $\mathcal{T}_e$ is the set of all elements crossed by $\widehat{X}(\xi, t^{n+1}; t^{n+1} - s)$ for any $\xi \in e$. Noting that for each edge $e \in \mathcal{E}_K$ we have

$$\sum_{K'} \int_e \Delta s_{K'}^{\xi}\ d\xi = |e| \Delta t,$$

from definition (34) the coefficients $\alpha_{K',e}$ are nonnegative numbers such that $\sum_{K'} \alpha_{K',e} = 1$. Furthermore, in the case of a velocity field that satisfies exactly the discrete divergence free constraint (6), the quantities $\Delta s_{K'}^{\xi}$ and $\alpha_{K',e}$ can be computed exactly starting from the piecewise constant representation of the vector field given in this case by the Raviart Thomas reconstruction.

The proof of monotonicity for the piecewise constant case now proceeds by showing that, using definition (33) in (30), and rearranging the sums appropriately, c_K^{n+1} is given by a linear combination of $c_{K'}^n$ with nonnegative

coefficients. This result can be readily proved in the case of sufficiently small time step and Courant number, along the lines of basic monotonicity proofs for upwind based schemes. In order to prove a similar result in the case of larger Courant numbers, it is useful to introduce the following sets

$$\mathcal{E}_K^+ = \{e \in \mathcal{E}_K : \sigma_{K,e} u_e \geq 0\}, \quad \mathcal{E}_K^- = \{e \in \mathcal{E}_K : \sigma_{K,e} u_e < 0\},$$

which represent the outflow and inflow boundaries of K, respectively. We also introduce the two following subsets of $\mathcal{T}_e$:

$$\mathcal{T}_K^+ = \bigcup_{e \in \mathcal{E}_K^+} \mathcal{T}_e, \qquad \mathcal{T}_K^- = \bigcup_{e \in \mathcal{E}_K^-} \mathcal{T}_e.$$

Clearly, $\mathcal{E}_K = \mathcal{E}_K^+ \cup \mathcal{E}_K^-$ and this fact can be used to reformulate (30) as

$$\begin{aligned} c_{0,K}^{n+1} = c_{0,K}^n & - \sum_{e \in \mathcal{E}_K^+} \frac{|u_e||e|\Delta t}{|K|} \sum_{K' \in \mathcal{T}_e} \alpha_{K',e} c_{0,K'}^n \\ & + \sum_{e \in \mathcal{E}_K^-} \frac{|u_e||e|\Delta t}{|K|} \sum_{K' \in \mathcal{T}_e} \alpha_{K',e} c_{0,K'}^n \\ = c_{0,K}^n & - \sum_{K' \in \mathcal{T}_K^+} \sum_{e \in \mathcal{E}_K^+} \frac{|u_e||e|\Delta t}{|K|} \alpha_{K',e} c_{0,K'}^n \\ & + \sum_{K' \in \mathcal{T}_K^-} \sum_{e \in \mathcal{E}_K^-} \frac{|u_e||e|\Delta t}{|K|} \alpha_{K',e} c_{0,K'}^n. \end{aligned} \tag{35}$$

For simplicity, we make now the assumption that $K \notin \mathcal{T}_K^-$, which excludes the case of very high Courant numbers or flows with very strong deformation (i.e., high Lipschitz numbers according to the definition in [41]). The monotonicity proof can in principle be extended to cover also these cases, but the above assumption greatly simplifies the proof. Furthermore, independently of this restriction one has $\mathcal{T}_K^+ = \{K\} \cup (\mathcal{T}_K^+ \cap \mathcal{T}_K^-)$. These facts are used to rearrange the sums on the right hand side of (35) as a linear combination of cell averages $c_{0,K'}^n$, so as to obtain

$$\begin{aligned} c_{0,K}^{n+1} = & \left(1 - \sum_{e \in \mathcal{E}_K^+} \frac{\Delta t |u_e||e|}{|K|} \alpha_{K,e}\right) c_{0,K}^n \\ & + \sum_{K' \in (\mathcal{T}_K^- \cap \mathcal{T}_K^+)} \frac{\Delta t}{|K|} \left(\sum_{e \in \mathcal{E}_K^-} |u_e||e| \alpha_{K',e} - \sum_{e \in \mathcal{E}_K^+} |u_e||e| \alpha_{K',e} \right) c_{0,K'}^n \\ & + \sum_{K' \in (\mathcal{T}_K^- \setminus \mathcal{T}_K^+)} \frac{\Delta t}{|K|} \sum_{e \in \mathcal{E}_K^-} |u_e||e| \alpha_{K',e} c_{0,K'}^n \end{aligned} \tag{36}$$

The proof of monotonicity is achieved if one can prove that all the coefficients of $c_{0,J}^n$ in the right hand side of (36) are non negative and sum up to one. The value of their sum can be obtained by taking $c_{0,J}^n = 1$ for all

elements J in the right hand side of (36) and tracing back the steps leading from (35) to (36). Since $\sum_{K' \in \mathcal{T}_e} \alpha_{K',e} = 1$, and using the fact that

$$\frac{\Delta t}{|K|} \sum_{e \in \mathcal{E}_K} \sigma_{K,e} |u_e||e| = \frac{\Delta t}{|K|} \Big[\sum_{e \in \mathcal{E}_K^-} |u_e||e| - \sum_{e \in \mathcal{E}_K^+} |u_e||e| \Big] = 0$$

because the discrete velocity field has been assumed to be divergence free (see equation (6)), the sum of the coefficients in the right hand side of (36) yields exactly one. These coefficients are also non negative. This is obvious for the third term in the sum in (36). For the first term, non negativity can be proven rigorously using the definition of $s_{K'}^{\xi}$ and exploiting again the assumption of a piecewise constant Raviart-Thomas reconstruction of the velocity field over each element. For the second term, non negativity is ensured by the fact that, for reasonably accurate approximations of the characteristic lines one has $\alpha_{K',e'} \geq \alpha_{K',e''}$ if $e' \in \mathcal{E}_K^-, e'' \in \mathcal{E}_K^+$. This allows to write that, for each $K' \in (\mathcal{T}_K^- \cap \mathcal{T}_K^+)$,

$$\begin{aligned} &\sum_{e' \in \mathcal{E}_K^-} |u_{e'}||e'| \alpha_{K',e'} - \sum_{e'' \in \mathcal{E}_K^+} |u_e''||e''| \alpha_{K',e''} \\ &\geq \min_{e' \in \mathcal{E}_K^-} \alpha_{K',e'} \Big[\sum_{e \in \mathcal{E}_K^-} |u_e||e| - \sum_{e \in \mathcal{E}_K^+} |u_e||e| \Big]. \end{aligned}$$

Using again the fact that the velocity field has discrete divergence equal to zero, non negativity for these coefficients follows as well.

5 Numerical experiments

In this section, the accuracy and stability of the SLDG method will be demonstrated in the numerical solution of two–dimensional benchmark test cases for passive tracer advection. In particular, solid body rotation and deformational flow tests will be considered, for which analytic solutions are available. The behaviour of the solution provided for these tests by the SLDG method will be compared with the results achieved in the same tests by its 'parent' methods, e.g. the standard, non conservative semi-Lagrangian (SL) method and the classical Runge–Kutta Discontinuous Galerkin (RKDG) method proposed and analyzed in [9]. In our opinion, these comparisons highlight several attractive properties of the SLDG formulation, which appears to merge effectively the SL and DG methods without any loss in accuracy or computational efficiency, while avoiding the most unpleasant shortcomings of the SL approach (loss of mass conservation, potential loss of accuracy at low Courant numbers) and of the DG approach (severe stability restrictions), respectively. Furthermore, the FCT based monotonization approach described in Sect. 4 appears to be superior to the slope limiting approach proposed in [8], [10] and does not display excessive sharpening of smooth profiles reported e.g. in [39] for more traditional applications of FCT. In particular, the idea of retaining the higher order degrees of freedom in the computation of the monotonized flux for the piecewise constant component of c_h^n is highly beneficial to the overall quality of the computed approximate solution. In

all the tests, the numerical solution is compared to the analytic one after four full rotations, at time level $T_{fin} = 4000$ s, and the following error norms are computed: $||u(T_{fin}) - u_h(T_{fin})||_{L^2(\Omega)}/||u(T_{fin})||_{L^2(\Omega)}$ and $||u(T_{fin}) - u_h(T_{fin})||_{L^\infty(\Omega)}/||u(T_{fin})||_{L^\infty(\Omega)}$. Moreover, we evaluate the *dissipation error* and the *dispersion error* as defined in [3], [43]. All the compared methods were coded using the `MATLAB` software environment for the purpose of this preliminary assessment. For the SL and SLDG runs, the backward trajectories were approximated by using the backward Euler method with substepping (see e.g. [38]).

5.1 Solid body rotation

For the solid body rotation test, a stationary velocity field was used, representing a rotating flow with frequency $\omega = 2\pi/1000$ s$^{-1} = 6.2832\text{e}-03$ s^{-1} around the point $(1,1)$ on the spatial domain $\Omega = (0,2)^2$. The initial datum was taken to be either a compactly supported C^3 function with the shape of a cosine hill or a piecewise constant, discontinuous function with the same support.

5.1.1 Experimental convergence analysis

In order to test the accuracy of the proposed SLDG method, we consider the standard test case of solid body rotation with smooth initial datum, namely a compactly supported C^3 function with the shape of a cosine hill, and we switch off the FCT limiter. We consider four unstructured computational grids of varying amplitude h, while keeping constant the Courant number. More specifically, we set the time step in order to mantain the maximum Courant number $C = 0.25$. Numerical quadratures are performed by setting $L_e = 2$, $L_f = 3$ and $M = 2$ in (16). Characteristics of the computational grids are summarized in Table 1 while numerical results are shown in Tab. 2.

h	N_{el}	$dofs$	Δt
$h = 0.1$	1372	4116	1.25
$h = 0.05$	5458	16374	0.625
$h = 0.033$	12222	36666	0.416
$h = 0.025$	22172	66516	0.312

Table 1: Computational grids for the convergence test.

The experimental convergence rates derived from Table 2 are $2.5, 2.6$ in the L^2, L^∞ norms, respectively. Analogous results, here omitted, have been obtained in the L^1 norm.

5.1.2 Behaviour at low Courant number

It is interesting to compare the results summarized in Tab. 2 with the analogous ones obtained using the SL and RKDG formulations under the same working conditions ($C = 0.25$). Tab. 3 refers to the solution computed

	Rel. L^2 error	Rel. L^∞ error	Dissipation error	Dispersion error	Min
h=0.1	3.53e-01	4.07e-01	1.96e-02	7.77e-02	-4.51e-01
h=0.05	1.24e-01	1.49e-01	1.51e-03	1.11e-02	-2.73e-01
h=0.033	5.58e-02	6.82e-02	1.96e-04	2.39e-03	-1.21e-01
h=0.025	2.73e-02	3.18e-02	3.36e-05	5.87e-04	-5.37e-02

Table 2: Convergence test for SLDG without FCT limiter: results after 4 full rotations of a smooth profile at $C = 0.25$.

by the SL method on three computational grids with $\mathbb{P}_2$ reconstruction, $h = \{0.1, 0.05, 0.025\}$ and $dofs = \{2825, 11077, 44665\}$.

	Rel. L^2 error	Rel. L^∞ error	Dissipation error	Dispersion error	Min
h=0.1	7.42e-01	7.13e-01	1.02e-01	1.74e+00	-7.00e-01
h=0.05	5.18e-01	4.86e-01	1.77e-02	8.80e-01	-1.08e+00
h=0.025	2.29e-01	2.14e-01	1.16e-03	1.75e-01	-6.87 e-01

Table 3: Convergence test for SL: results after 4 full rotations of a smooth profile at $C = 0.25$.

Tab. 4 refers to the solution computed by the RKDG method without slope limiting on two computational grids with $\mathbb{P}_1$ finite elements, $h = \{0.1, 0.05\}$ and $dofs = \{4116, 16374\}$.

	Rel. L^2 error	Rel. L^∞ error	Dissipation error	Dispersion error	Min
h=0.1	3.47e-01	3.99e-01	2.48e-02	6.91e-02	-2.74e-01
h=0.05	1.15e-01	1.41e-01	2.22e-03	8.55e-03	-1.56e-01

Table 4: Convergence test for RKDG without slope limiting: results after 4 full rotations of a smooth profile at $C = 0.25$.

These results show that at low Courant number the SLDG method does not suffer from the error amplification that is typical of SL methods (see e.g. the analysis in [14]), while its accuracy is completely comparable to that of the RKDG method.

It is now important to address the effect of limiting procedures on the computed solution. With this aim, we compare the performance of SLDG method with FCT monotonization and RKDG method with slope limiting monotonization. Results are summarized in Tab. 5 for the smooth advected profile and in Tab. 6 for the discontinous advected profile, respectively. Both cases were computed at resolution $h = 0.1$.

It is remarkable to notice that the FCT strategy applied to SLDG is far less diffusive than the slope limiting procedure used in the RKDG formulation. This can be seen also in the plots of the solutions displayed in Fig. 5.

	Rel. L^2 error	Rel. L^∞ error	Dissipation error	Dispersion error
SLDG	4.28e-01	5.51e-01	6.24e-02	8.00e-02
RKDG	8.74e-01	9.23e-01	4.36e-01	1.59e-01

Table 5: Comparison of SLDG and RKDG with monotonization: results after 4 full rotations of a smooth profile at $C = 0.25$.

	Rel. L^2 error	Rel. L^∞ error	Dissipation error	Dispersion error
SLDG	4.48e-01	6.03e-01	2.18e-01	2.62e-01
RKDG	8.73e-01	8.98e-01	1.34e-00	4.88e-01

Table 6: Comparison of SLDG and RKDG with monotonization: results after 4 full rotations of a discontinuous profile at $C = 0.25$.

It can be observed as well that the SLDG solution does not display excessive sharpening of smooth profiles reported e.g. in [39] for more traditional applications of FCT.

These results suggest that the present FCT approach, beyond its application in conjunction to SLDG, could also be a useful improvement of monotonization techniques in the framework of generak DG approximations.

5.2 Behaviour at high Courant number

In this section the numerical performance of the SLDG formulation at $C = 3$ is analyzed. Results are summarized in Tab. 7 for the smooth advected profile without monotonization, computed at resolution $h = 0.05$. The number of elements and degrees of freedom is the same as reported in the section on low Courant number results. The results of SLDG are compared to those of a standard SL method with continuous $\mathbb{P}_2$ reconstruction. As it is well known, the SL solution is quite sensitive to the trajectory approximation technique. Thus, we report results in two extreme cases of simple Euler approximation with substepping, indicated as SL(a), and of semi-Lagrangian advection computed using the analytical trajectory, indicated as SL(b). On the other hand, for the SLDG method only the simple Euler approximation has been used. It can be seen that the results of SLDG are much less sensitive to the trajectory approximation method and that the SLDG errors are comparable to those of SL(b), while they are superior to SL(a). This greater accuracy of SLDG, however, corresponds to a potentially higher computational cost, due to the fact that numerical solution does not only involve reconstructions at the foot of the characteristic lines, but along these as well.

5.3 Deformational flow tests

The deformational flow tests considered were the non divergent vortical

	Rel. L^2 error	Rel. L^∞ error	Dissipation error	Dispersion error
SLDG	7.31e-02	7.20e-02	2.55e-04	4.13e-03
SL(a)	2.45e-01	2.44e-01	6.61e-03	1.95e-01
SL(b)	7.75e-02	7.40e-02	5.51e-04	1.96e-02

Table 7: Comparison of SLDG with $\mathbb{P}_1$ reconstruction and SL with continuous $\mathbb{P}_2$ reconstruction: results after 4 full rotations of a smooth profile at $C = 3$.

velocity field introduced in [11], which has been used by many authors to assess the accuracy of advection schemes, see e.g. [34], [35], and the well known test proposed by P. Smolarkiewicz in [40]. For the non divergent vortex of [11], a circular domain of radius $R = 3$ was considered, which was discretized with a triangular mesh composed of 2352 elements with $dofs = 7056$. The initial datum was given by a function taking two different constant values on the upper and lower half of the computational domain, respectively, with a sharp transition zone in the middle. The zero order degrees of freedom representing cell averages are displayed in Fig. 6, as computed by the monotonized SLDG and RKDG schemes, at $C = 2$ and at $C = 0.3$, respectively. It can be observed that the monotonization approach proposed for SLDG leads to a much sharper interface and to much greater detail in the vortex roll-up zone, which is consistent with the error statistics shown in Table 8.

	Rel. L^2 error	Rel. L^1 error	Dissipation error	Dispersion error
SLDG	2.24e-01	1.05e-01	8.04e-04	1.2185
RKDG	3.55e-01	1.96e-01	9.80e-3	3.0571

Table 8: Errors for the SLDG solution (at $C = 2$) and RKDG solution (at $C = 0.3$)in the Doswell deformation flow test case.

The SLDG solution for the deformation flow proposed in [40] is displayed in Fig. 7, along with a reference solution computed using the standard RKDG method with higher order elements and a much smaller timestep. It can be observed that the SLDG method is quite effective in reproducing very similar results using a much longer time step. The effective reduction of the associated computational cost can only be estimated precisely once the optimal time discretization approach will have been identified.

6 Coupling the SLDG method to discrete models of divergent flow

Divergent flows or two dimensional free surface flows are often considered in applications to realistic environmental problems. In these cases the SLDG method proposed in the present article should be coupled to an appropriate

discretization of the continuity equation. For sake of simplicity, this problem will be described here in greater detail in the case of a two dimensional divergent flow. Consider the coupled system

$$\frac{\partial H}{\partial t} + \nabla \cdot \Big(H \mathbf{u} \Big) = 0, \tag{37}$$

$$\frac{\partial (cH)}{\partial t} + \nabla \cdot \Big(cH \mathbf{u} \Big) = 0 \tag{38}$$

where $\mathbf{u}$ is the velocity field, H is the thickness of a homogeneous two-dimensional layer of fluid and c is the concentration of an advected tracer. System (37)-(38) enjoys the basic property that setting $c = 1$ in (38), equation (37) is recovered. If this property of compatibility or *consistency with continuity* is not preserved also at a discrete level, effective loss of mass conservation and monotonicity arise, even for fully conservative discretizations of (37), see e.g. the discussion in [21], [27], [28], [39]. The inaccuracies resulting from neglecting this issue in realistic atmospheric chemistry models have been analyzed in [24].

In many mass conservative environmental models (see e.g. [4], [5], [6], [32]), the continuity equation (37) is usually discretized using a finite volume method as

$$H_{0,K}^{n+1} = H_{0,K}^{n} - \sum_{e \in \mathcal{E}_K} \frac{\sigma_{K,e} |u_e| |e| \Delta t}{|K|} H_e^n .$$

Here, the same notation as in Sect. 2 was used and u_e denotes a discrete velocity field. In many applications, for the sake of efficiency, equation (6) is the result of a semi-implicit discretization, so that indeed the velocities involved are to be interpreted as velocity values at an intermediate time step $u_e = u_e^{n+\frac{1}{2}}$ and switching to a different numerical method to ensure consistency might require extensive reformulation of the available numerical models. Thus, it is convenient to discretize (38) so that consistency with (6) is achieved automatically.

The discretization of the tracer equation by the SLDG method can be extended to the divergent case as follows. The equation for the degree of freedom corresponding to the mean over each element can be discretized as

$$\begin{aligned} H_{0,K}^{n+1} c_{0,K}^{n+1} \quad &= H_{0,K}^{n} c_{0,K}^{n} \\ &- \sum_{e \in \mathcal{E}_K} \frac{\sigma_{K,e}}{|K|} H_e^n F_e^0 - \sum_{e \in \mathcal{E}_K} \frac{\sigma_{K,e}}{|K|} C_e H_e^n \left[\sum_{j=1}^{2} F_e^j \right] . \end{aligned} \tag{39}$$

It is to be remarked here that this equation is entirely analogous to the equation for $c_{0,K}^{n+1}$ in (16). For any reasonable definition of the numerical fluxes, this expression will yield exactly equation (6) in the case of constant $c_{0,K}^n$, so that discrete consistency is granted. It should be remarked, however, that the divergence free property of the flow was essential for the present derivation of monotonic low order fluxes F_e^0. Thus, the presently available proof of monotonicity does not hold in the divergent case and needs to be extended appropriately, while on the other hand a non monotonic version of the scheme can be extended to the divergent case straightforwardly.

7 Open issues and further developments

The main open issue with respect to the SLDG method at this stage appears to be the characterization of the accuracy required in the space-time quadrature formulas introduced in Sect. 2.4. A precise evaluation of the relative accuracy and efficiency of the SLDG method compared to other more mature methods will only be feasible once this point has been properly addressed. The accuracy required in the quadrature formulas for the approximate computation of the fluxes and volume integrals in equation (8) appears to be related to the local Courant number, in the sense that, for low Courant numbers, a smaller number of quadrature points appears to be necessary to achieve the same accuracy. One possibility to achieve greater computational efficiency could be to choose the number of quadrature points locally in space and time as a function of the Courant number.

Finally, a major theoretical development that also appears feasible is to provide a convergence and stability proof for the SLDG method along the lines of [14], which should be able to give a more rigorous basis to the empirical finding on the better convergence rate of the SLDG formulation compared to the classical SL approach discussed in Sect. 5.

8 Conclusions

The SLDG discretization approach for the scalar advection equation has been introduced, combining the accuracy and flexibility of the DG method with the computational efficiency and robustness of semi - Lagrangian techniques. Unconditional stability of the proposed discretization was proven in the von Neumann sense for the one dimensional case. A monotonization technique has also been introduced, based on the Flux Corrected Transport approach, which yields a multidimensional monotonic scheme for the piecewise constant component of the computed solution, while reducing the numerical diffusion of monotonization approaches more common in the Discontinuous Galerkin framework. The accuracy and stability of the method have been demonstrated by two dimensional tracer advection tests. In particular, the comparison with results obtained by standard semi - Lagrangian and Discontinuous Galerkin methods has shown that SLDG merges effectively the most desirable properties of both approaches, while avoiding their most remarkable shortcomings. More thourough theoretical analysis and further testing of the proposed approach are currently being undertaken, as well as its extension to tracer transport in divergent flows and to the solution of nonlinear systems of conservation laws.

Acknowledgements

We thank J. Behrens, E.S. Gross, T. Ringler, G. Rosatti and W. Sawyer for several discussions on conservative semi-Lagrangian methods over the last few years. The helpful comments of F. Giraldo on a preliminary version of this paper are kindly acknowledged. The numerical method presented here

is currently being investigated in the framework of the PhD thesis of one of the authors (MR), under the supervision of the other two (LB, RS).

References

[1] A. Arakawa and V. Lamb. A potential enstrophy and energy conserving scheme for the shallow water equations. *Monthly Weather Review*, 109:18–136, 1981.

[2] J.R. Bates and A. McDonald. Multiply-upstream, semi-Lagrangian advective schemes: analysis and application to a multilevel primitive equation model. *Monthly Weather Review*, 110:1832–1842, 1982.

[3] R. Bermejo and A. Staniforth. The conversion of semi-lagrangian advection schemes to quasi-monotone schemes. *Monthly Weather Review*, 120:2622–2632, 1992.

[4] L. Bonaventura. The ICON project: Development of a unified model using triangular geodesic grid. In *Proceedings of the ECMWF Annual Seminar on Development in Numerical Methods for Atmosphere and Ocean Modeling*. ECMWF, 2004.

[5] L. Bonaventura, L. Kornblueh, T. Heinze, and P. Ripodas. A semi-implicit method conserving mass and potential vorticity for the shallow water equations on the sphere,. *International Journal of Numerical Methods in Fluids*, 47:863–869, 2005.

[6] V. Casulli and R.A. Walters. An unstructured grid, three-dimensional model based on the shallow water equations. *International Journal of Numerical Methods in Fluids*, 32:331–348, 2000.

[7] G. Chavent and B. Cockburn. Consistance et stabilite des schemas LRG pour les lois de conservation scalaires. INRIA Rapport de Recherche 710, INRIA, 1987.

[8] B. Cockburn, S. Hou, and C.W. Shu. The Runge-Kutta Local Projection Galerkin Finite Element Method for conservation laws IV: the multidimensional case. *Mathematics of Computation*, 54 (190):545–581, 1990.

[9] B. Cockburn and C.W. Shu. The runge-kutta local projection P1 Discontinuous Galerkin method for scalar conservation laws. *Mathematical Modelling and Numerical Analysis*, 25:337–361, 1991.

[10] B. Cockburn and C.W. Shu. The Runge-Kutta Discontinuous Galerkin method for conservation laws, V. *Journal of Computational Physics*, 141:198–224, 1998.

[11] C. A. Doswell. A kinematic analysis of frontogenesis associated with a nondivergent vortex. *Journal of the Atmospheric Sciences*, 41:1241–1248, 1984.

[12] J.K. Dukowicz and J.R. Baumgardner. Incremental remapping as a transport/advection algorithm. *Journal of Computational Physics*, 160:318–335, 2000.

[13] R.E. Ewing and H. Wang. A summary of numerical methods for time-dependent advection-dominated partial differential equations. *Journal of Computational and Applied Mathematics*, 128:423–445, 2001.

[14] M. Falcone and R. Ferretti. Convergence analysis for a class of semi-lagrangian advection schemes. *SIAM Journal of Numerical Analysis*, 35:909–940, 1998.

[15] M. Fey. Ein echt mehrdimensionales Verfahren zur Lösung der Eulergleichungen. Dissertation 10034, ETH, 1993.

[16] M. Fey. Multidimensional upwinding. part i: The method of transport for solving the Euler equations. *Journal of Computational Physics*, 143:159–172, 1998.

[17] M. Fey. Multidimensional upwinding. part ii: Decomposition of the Euler equations into advection equations. *Journal of Computational Physics*, 143:181–199, 1998.

[18] P. Frolkovic. Flux-based method of characteristics for contaminant transport in flowing groundwater. *Computing and Visualization in Science*, 5:73–83, 2002.

[19] P. Frolkovic. Flux-based methods of characteristics for coupled transport equations in porous media. *Computing and Visualization in Science*, 6:173–184, 2004.

[20] S. Gravel and A. Staniforth. A mass-conserving semi-lagrangian scheme for shallow water equations. *Monthly Weather Review*, 122:243–248, 1994.

[21] E.S. Gross, L. Bonaventura, and G. Rosatti. Consistency with continuity in conservative advection schemes for free-surface models. *International Journal of Numerical Methods in Fluids*, 38:307–327, 2002.

[22] C.W. Hirt, A.A. Amsden, and J.L. Cook. An arbitrary Lagrangian-Eulerian computing method for all flow speeds. *Journal of Computational Physics*, 14:227–245, 1979.

[23] L.W. Horowitz, S. Walters, D.L. Mauzerall, L.K. Emmons, P.J. Rasch, C. Granier, X. Tie, J.F. Lamarque, M.G. Schultz, and G.P. Brasseur. A global simulation of tropospheric ozone and related tracers: Description and evaluation of MOZART, version 2. *Journal of Geophysical Research*, 108:4784–4802, 2003.

[24] P. Jöckel, R. von Kuhlmann, M.G. Lawrence, B. Steil, C.A.M. Brenninkmeijer, P.J. Crutzen, P.J. Rasch, and B. Eaton. On a fundamental problem in implementing flux-form advection schemes for tracer transport in 3-dimensional general circulation and chemistry transport models. *Quarterly Journal of the Royal Meteorological Society*, 127:1035–1052, 2001.

[25] J.P.R. Laprise and R. Plante. A class of semi-Lagrangian integrated-mass (SLIM) numerical transport algorithms. *Monthly Weather Review*, 123:553–565, 1995.

[26] B.P. Leonard, A.P. Lock, and M.K. MacVean. Conservative explicit unrestricted-time-step multidimensional constancy-preserving advection schemes. *Monthly Weather Review*, 124:2588–2606, November 1996.

[27] R.J. Leveque. High-resolution conservative algorithms for advection in incompressible flow. *SIAM Journal of Scientific Computing*, 33(2):627–665, April 1996.

[28] S.J. Lin and Richard B. Rood. Multidimensional flux-form semi-Lagrangian transport schemes. *Monthly Weather Review*, 124:2046–2070, September 1996.

[29] W.H. Lipscomb and T.D. Ringler. An incremental remapping transport scheme on a spherical geodesic grid. *Monthly Weather Review*, To appear, 2005.

[30] B. Machenhauer and M. Olk. The implementation of the semi-implicit scheme in cell-integrated semi-Lagrangian models. *Atmosphere-Ocean*, XXXV(1):103–126, March 1997.

[31] B. Machenhauer and M. Olk. Design of a semi-implicit cell-integrated semi-Lagrangian model. In *MPI workshop on conservative transport schemes: 2-3 June 1997*, pages 76–85. MPI Report No. 265, July 1998.

[32] E. Miglio, A. Quarteroni, and F. Saleri. Finite element approximation of quasi-3d shallow water equations. *Comp. Methods in Applied Mechanics and Engineering*, 174:355–369, 1999.

[33] K. W. Morton. On the analysis of finite volume methods for evolutionary problems. *SIAM Journal of Numerical Analysis*, 35:2195–2222, 1998.

[34] R.D. Nair, J. Coté, and A. Staniforth. Monotonic cascade interpolation for semi-lagrangian advection. *Quarterly Journal of the Royal Meteorological Society*, 125:197–212, 1999.

[35] R.D. Nair and B. Machenhauer. The mass-conservative cell-integrated semi-Lagrangian advection scheme on the sphere. *Monthly Weather Review*, 130:649–667, 2002.

[36] A. Priestley. A quasi-conservative version of semi-Lagrangian advection scheme. *Monthly Weather Review*, 121:621–629, 1993.

[37] Alfio Quarteroni and Alberto Valli. *Numerical approximation of partial differential equations*. Springer Verlag, 1994.

[38] G. Rosatti, L. Bonaventura, and D. Cesari. Semi-implicit, semi-Lagrangian environmental modelling on cartesian grids with cut cells. *Journal of Computational Physics*, 204:353–377, 2005.

[39] C. Schär and P.K. Smolarkiewicz. A synchronous and iterative flux-correction formalism for coupled transport. *Journal of Computational Physics*, 128:101–120, 1996.

[40] P.K. Smolarkiewicz. A fully multidimensional positive definite advection transport algorithm with small implicit diffusion. *Journal of Computational Physics*, 54:325–362, 1984.

[41] P.K. Smolarkiewicz and J. Pudykiewicz. A class of semi-Lagrangian approximations for fluids. *Journal of the Atmospheric Sciences*, 49:2082–2096, 1992.

[42] A. Staniforth and J. Coté. Semi-lagrangian integration schemes for atmospheric models-a review. *Monthly Weather Review*, 119:2206–2223, 1991.

[43] L.L. Takacs. A two step scheme for the advection equation with minimized dissipation and dispersion errors. *Monthly Weather Review*, 113:1050–1065, 1985.

[44] C. Timmreck. Three-dimensional simulation of stratospheric background aerosol: First results of a multiannual general circulation model simulation. *Journal of Geophysical Research*, 106:28313–28332, 2001.

[45] S. Zalesak. Fully multidimensional Flux Corrected Transport algorithms for fluids. *Journal of Computational Physics*, 31:335–362, 1979.

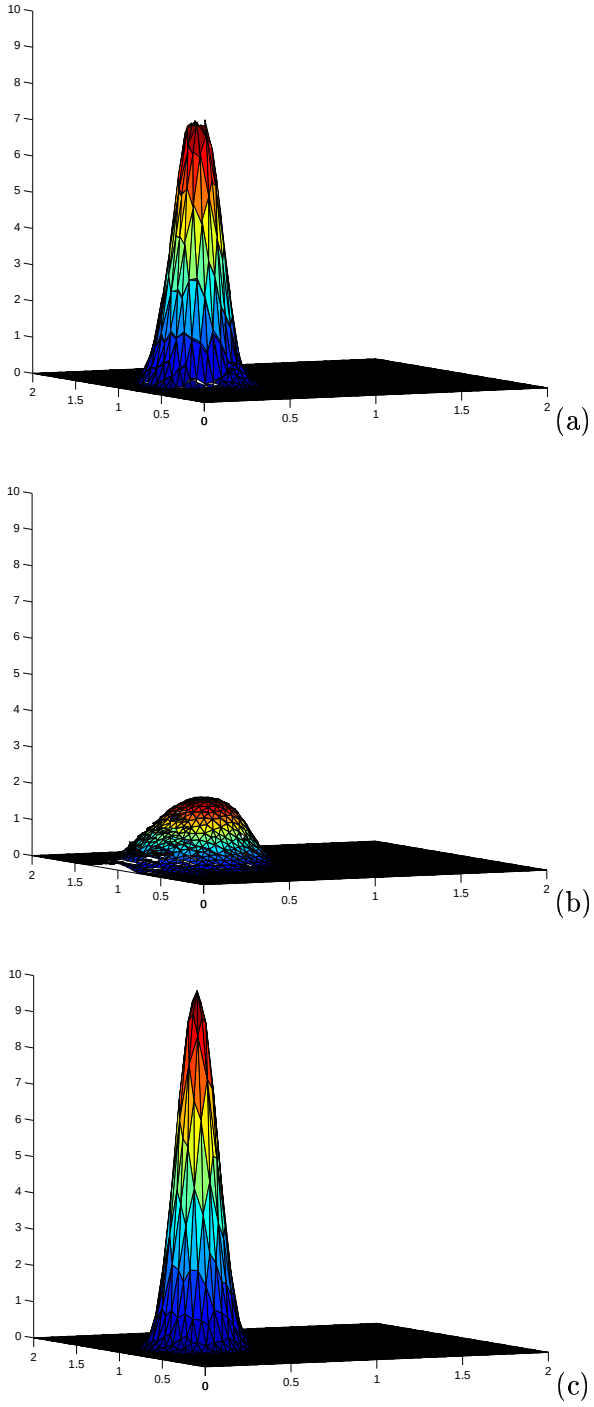

Figure 5: Monotonized solutions in the solid body rotation test case at $C = 0.25$. SLDG solution computed with $\mathbb{P}_1$ elements (a) RKDG solution computed with $\mathbb{P}_1$ elements (b) and analytic solution (c).

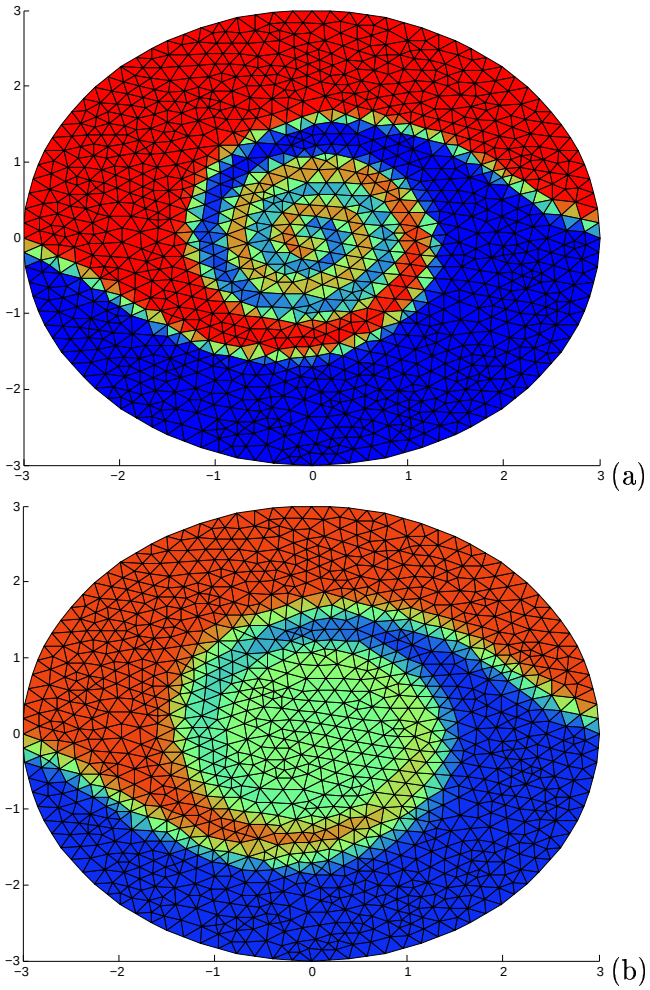

Figure 6: Solutions in the Doswell deformation flow test case. SLDG solution computed with $\mathbb{P}_1$ elements at $C = 2$ (a) and RKDG reference solution computed with $\mathbb{P}_1$ elements at $C = 0.3$ (b).

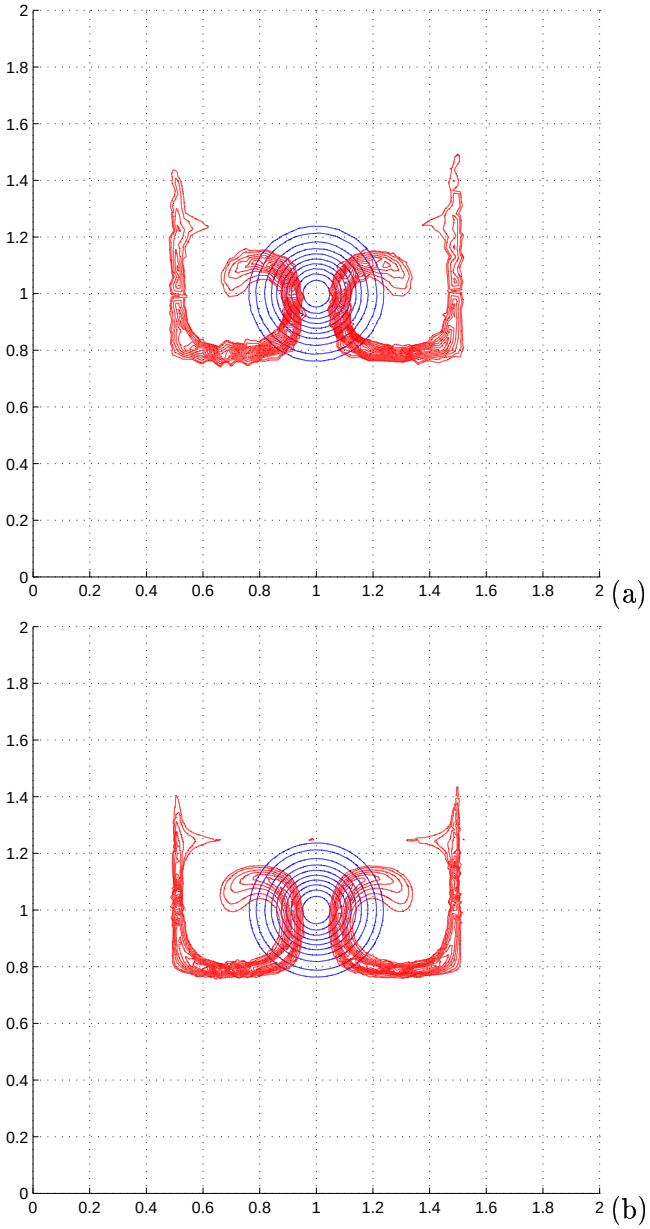

Figure 7: Solutions in the Smolarkiewicz deformation flow test case. SLDG solution computed with $\mathbb{P}_1$ elements at maximum Courant number 4 (a) and reference RKDG solution computed with $\mathbb{P}_2$ elements (b). Red contours: numerical solution; blue contours: inital datum.